3-1-1990

Effects of Auxiliary Heat Treatment on Flame-Cutting Procedures for Steel Plates

Bruce R. Somers

Howard Smith

Rajan Varughese

Alan W. Pense

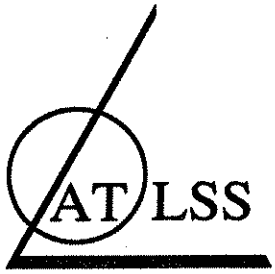

ADVANCED TECHNOLOGY FOR
LARGE
STRUCTURAL SYSTEMS

Lehigh University

EFFECTS OF AUXILIARY HEAT TREATMENT ON FLAME-CUTTING PROCEDURES FOR STEEL PLATES

by

Bruce R. Somers
Somers Consultants, Bethlehem, PA

Howard Smith
ATLSS REU Program
and Lafayette College Student

Rajan Varughese
ATLSS Research Associate

Alan W. Pense
Dean, College of Engineering and Applied Science
Lehigh University

ATLSS Report No. 90 - 03

March, 1990

ATLSS Engineering Research Center
Lehigh University
117 ATLSS Dr., Imbt Laboratories
Bethlehem, PA 18015
(215) 758-3535

An NSF Sponsored Engineering Research Center

ABSTRACT

Flame-cutting of steel plates can introduce metallurgically hard heat-affected zones (HAZ) of low toughness. These hard HAZ's can adversely affect the serviceability of flame-cut surfaces. This report discusses an evaluation of an auxiliary heating device which, when used in conjunction with a standard flame-cutting apparatus, can improve the serviceability of the cut surface.

One-inch and two-inch thick flame-cut samples of A588 steel were prepared using three different cutting treatments including cutting with auxiliary pre- and post-heating, cutting with auxiliary post-heating only, and cutting with no auxiliary heating. The auxiliary heat was applied to the cutting process using a proprietary fixture designed by Roussey Associates of Downingtown, PA. Each cutting treatment was applied at both a fast and a slow cutting speed. Surface hardness tests showed, as expected, that within the same composition and thickness, the hardest flame-cut surfaces occurred at the faster cutting speed when no auxiliary heating was applied. The softest surface occurred at slow cutting speeds when both pre- and post-heating flames were applied. Microhardness traverses show the tempering effects of the auxiliary heat. As expected, the highest microhardness values were found in the two-inch samples cut with no auxiliary heat.

Bend tests were performed to determine the relative ductility and cracking resistance of the flame-cut surfaces. For the one-inch samples with pre- and post-heating at both cutting speeds, none or only very slight cracking was observed. Numerous slight cracks, however, were found when no auxiliary heat treatment was used. The two-inch thick plate cut with no auxiliary heat generated through cracks during bending. While pre- and post-heat treatments reduced the cracking severity in the two-inch plate, numerous slight cracks were still seen, even at slow cutting speeds.

The metallurgical effects from flame cutting were observed on metallographic sections using a light optical microscope. Without pre- or post-heat, the HAZ consisted of martensite at the surface with pearlite and ferrite further beneath the flame-cut surface. The post-heat HAZ consisted of a more bainitic structure at the surface while the pre- and post-heat HAZ had fine pearlite near the surface, although tempered martensite is more characteristically found in the HAZ's of production size cuts using this auxiliary heat procedure. Further below the flame-cut surface, a coarser pearlite-ferrite mixture characteristic of the unaffected base metal was observed.

On the basis of these evaluations, the use of the auxiliary heating device enhances the serviceability of flame-cut surfaces in plate thicknesses of two inches and less.

ACKNOWLEDGEMENT

This study was sponsored by Roussey Associates, Downingtown, PA, as part of a Small Business Innovation grant from the U.S. Department of Energy.

TABLE OF CONTENTS

INTRODUCTION

Oxyfuel cutting is a technique widely used in cutting steel plates and strips. Typical uses of this method include shipbuilding, fabrication of structural sections, heavy equipment, machinery, pressure vessels, and storage tanks. During a typical oxyfuel cut a preheat flame heats the steel to initiate the oxidation reaction. An oxygen jet then oxidizes this metal and the resulting exothermic reaction provides enough heat to melt the steel and continue the cutting. The force of the oxygen jet also clears the area of molten metal and oxide.

While this method works well with plain carbon steels, higher carbon and alloy steels frequently require additional pre- or post-heat treatments to avoid cracking and toughness problems associated with the higher hardenability of these materials. A588 and other high-strength low-alloy (HSLA) steels, although not generally considered materials of higher hardenability in the normal sense, do contain alloy additions such as manganese, copper, nickel, chromium, vanadium, columbium, etc., and can transform to hard microstructures as a result of the severe thermal gradients produced by the oxyfuel cutting process. As a result, economical use of flame-cutting in situations involving high carbon steels and HSLA steels can be problematical.

The rapid heating and cooling associated with the flame cutting process can create high hardness, low toughness areas of martensite in the heat affected zone (HAZ) of the flame cut surface. This is similar to the HAZ formed in welding, where additional heat treatments - post weld heat treatments, frequently termed "stress relief" - are often used to avoid problems associated with cracking of this hardened zone. Additionally, several researchers (1-3) have suggested that a selective oxidation in the molten layer which reso-

lidifies on the cut surface often raises the level of carbon, further enhancing the hardenability of this region. The expansion and contraction associated with both the heating and cooling, and the metallurgical phase transformations that occur during the flame cutting, can also create residual stresses in the metal making it more susceptible to cracking. In fact, stress relief heat treatment or grinding away the martensitic edge can be used to avoid most of these problems. However, these solutions can be expensive.

An invention proposed by Roussey Associates of Downingtown, PA, which adds auxiliary pre- and post-heat flame jets to the standard flame cutting machine may also eliminate the above problems. The invention consists of a manifold which is supplied with an oxyfuel mixture that emerges at several nozzles along the length of the manifold; see Figure 1. The oxygen cutting jet is located between the auxiliary heating nozzles and the cutting position is therefore subjected to pre- and post-heating with the heating functions spread along the direction of the cut. This apparatus also allows for possible energy savings in that the entire plate would not have to undergo heat treatments, nor would the grinding processes be required. Also, having this entire series of jets on one manifold allows for greater cutting speed and potential for automation.

The intention of this report is to evaluate, through a variety of tests, the mechanical and metallurgical properties produced when various samples of A588 steel plates were cut with the Roussey Associates device.

PROCEDURE

The materials and cutting parameters were selected to be representative of cutting practices normal to the structural fabrication industry. Table I shows the identity and composition of the steels used. Two one inch thick A588 heats identified as 1A and 1B with carbon equivalents of 0.42 and 0.49 respectively were evaluated. A single heat of two inch thick A588 identified as 2A with a carbon equivalent of 0.49 was also evaluated. Table II shows the mechanical properties of these A588 materials as reported on their mill test certifications. Because of the rather high Charpy-V notch (CVN) values reported for heat 1A, a full CVN transition curve was determined to confirm these values; see Figure 2.

The A588 steel plates were flame cut in accordance with the schedules listed in Table III. Three treatments were employed: 1) cutting with auxiliary pre- and post-heat (PPH), 2) cutting with auxiliary post-heat only (PH), and 3) cutting with no auxiliary pre- or post-heat (NH). The one-inch plates were cut at both 10 and 15 inches per minute and the two-inch plate was cut at 8 and 13 inches per minute. For each of these thicknesses, treatments and cutting speeds, two six-inch lengths of the flame-cut surface were removed and prepared for bend tests. The bend specimen width was the thickness of the original plate and the specimen thickness was 3/8 inch. The specimens were tested in a guided bend fixture in accordance to Fig. 5.27.1A of AWS D1.1, with a 3/4 inch bend radius putting the flame-cut side in tension. The resulting bend specimens were then rated on a scale of 0 to 2, where a rating of 0 represents no significant observable cracking, 1 represents short cracks with visible openings and a rating of 2 represents a large crack across the entire width of the specimen; see Figure 3. Ratings between 0, 1, and 2 represent the relative severity of cracking.

One sample for each thickness, heat treatment, and cutting speed was also prepared for surface hardness measurements, microhardness traverses, and photomicrographs. Surface hardness measurements were taken in five locations along the sample flame-cut surface at the top, middle, and bottom. These readings were then averaged to obtain a Rockwell "C" (R_C) hardness number for each specimen.

The hardness indentations of the microhardness traverses were concentrated in the first 0.04 inch below the flame-cut surface in order to detect the steep hardness gradient at the surface; see Figure 4. However, the traverse extended to a total distance of 0.25 inch below the surface. In some of the latter microhardness work an attempt was made to evaluate the scatter in the recorded values by taking multiple readings at the same distance from the cut surface.

Metallographic specimens were removed from the mid-thickness of each cut plate and prepared in order to examine a transverse section perpendicular and adjacent to the flame-cut surface. Photomicrographs were taken of each sample showing the entire microstructure of each specimen including the surface, the HAZ, and the area further below the surface of the sample.

RESULTS

The results of the bend tests are summarized in Table IV. These ratings are by necessity semi-quantitative and are determined by visual inspection of the bend specimen after testing. In all cases the auxiliary heating improved the bend test behavior. In the one-inch thick material, the addition of both pre- and post-heat eliminated nearly all cracking in the bend test; whereas, in the two-inch thick material, the addition of pre- and post-heat, while it

did not completely eliminate cracking, did reduce the extent of cracking from through cracks to slight cracks. It is interesting to note that the bend test results appear to show little effect due to the speed of cutting over the range tested.

The results of the microhardness survey are shown in Figures 5 through 10. In all cases, the addition of auxiliary heat reduced the maximum hardness observed in the flame-cut HAZ, although not as markedly in the lower carbon equivalent heat 1A. Table V shows the typical variability of the data obtained in these microhardness surveys. As expected, the variability is greatest at the 0.01 to 0.02 inch depth where the hardness is changing steeply as a function of depth.

The results of the surface hardness tests are summarized in Figure 11 and 12. Again, clearly the addition of auxiliary heat reduced the surface hardness.

The photomicrographs of typical HAZ's for heats 1A and 2A are shown in Figures 13A through 13L.

DISCUSSION

The appropriateness of this bend and hardness test to determine the viability of this procedure in actual structural applications is a question that should be considered before proceeding. Wilson (4), in his report on thermal cutting of HSLA bridge steels prepared for AISI, selected these tests and has addressed this question. He infers that while the bend test is a severe test, it is useful in sorting out the influences of various processing variables. Nevertheless, it may not necessarily represent the expected performance in an actual structure. This was highlighted during the bend testing

of heat 1B when one of the samples cut with no auxiliary heat performed significantly better than the other within this group. Upon closer observation it was found that this specimen has two strategically placed gouges on the surface so that the major cracks that had been observed in the other specimens of this group were, in effect, distributed between these two gouge sites, causing an apparent slight relief of constraint and yielding a better bend test performance.

This is interesting in that a considerable amount of work has suggested that the fatigue resistance of a flame-cut surface is strongly influenced by the roughness of the cut (2, 5, 6). That is, a rougher surface gives poorer fatigue performance. Nevertheless the bend test is a standard test generally accepted as a means of gauging ductility.

It should be noted that most applications of the bend test utilize a specimen of relatively uniform mechanical properties. In this work the specimen represents a composite of properties and as such the toughness of the underlying base metal can play a significant role in the propagation or arrest of a crack initiated in the flame-cut surface. Thus, although this test can be useful to measure the effects of variables in the flame-cutting process, it may be possible that an especially tough base plate could mask some of these effects. This is likely why the results of the Heat 1A, a plate of good toughness, do not show the marked bend test improvement noted in Heat 1B. The as-cut Heat 1A already had fairly good bend performance without adding auxiliary heat.

As mentioned above, the fatigue resistance of a flame cut surface is strongly influenced by the roughness of the cut. It should be noted that close

visual examination of the cut surfaces revealed that within the same thickness and cutting speed, the application of the auxiliary heat had no detectable effect on the surface roughness of the cut.

The hardness test gives a definite quantitative result, although its application and relationship to service performance is also heavily dependent upon experience and empirical correlations. In this regard it has been suggested that a maximum flame-cut HAZ hardness of less than 350 HV (approximately equivalent to 360 Knoop or 36.5 R_C) has been associated with adequate ductility and crack resistance in service (7). The New York Department of Transportation has set a maximum flame-cut edge hardness of 30 R_C for ASTM A588 plate.

In comparing the bend test results for each sample thickness, it is seen (as might be expected) that the one-inch thick samples generally crack less than the thicker two-inch samples. Within each thickness the results indicate the effects of auxiliary heat and cutting speed are similar. The least cracking occurred in the samples cut with both pre- and post-heat flames. The most cracking is seen when no auxiliary heat treatment was applied. In both thicknesses of the higher carbon equivalent plates, through cracks occurred in the samples without heat treatment. The greatest improvement is seen when both auxiliary pre- and post-heat are applied at the cut.

The results of the microhardness traverses, as expected, show a reduction in maximum HAZ hardness as auxiliary heat treatments are added to the cutting procedure; see Figures 5-10. For two-inch, slow speed samples, Figures 9 and 10, the maximum Knoop hardness values are 543, 465, 354 for no auxiliary heat, auxiliary post-heat only, and auxiliary pre- and post-heat, respective-

ly. Because of the faster cooling involved with fast cutting speeds, assuming the heat input was constant, a higher maximum hardness would be expected in the surfaces cut at higher speeds. However this trend, although observed in the surface hardness readings, was not noted in the microhardness results. Nevertheless, the microhardness results clearly show an advantage of auxiliary heat is the reduction of hardness throughout the HAZ. In this regard, as expected, the addition of both pre- and post-heat appears to be more effective than the addition of post-heat only.

The microhardness surveys reveal the addition of auxiliary heat appears to be more effective when applied at slower speeds, as might be expected from heat flow and heat input considerations. In the one-inch plates, Figures 5 through 8, the suggested level of 350 HV is attained by the post-heat alone for all but the fast cutting speed of the heat 1B, the higher carbon equivalent plate. In this plate the application of both pre- and post-heat drops the hardness to below the 350 HV level. In the two-inch plates, only at the slower cutting speed with the application of both pre- and post-heat does the hardness drop to near the 350 HV level.

Surface hardness measurement results summarized in Figures 11 and 12 reinforce the previously discussed results. As above, the samples with no auxiliary heat treatment yielded the hardest surfaces, followed by post-heat, and finally pre- and post-heated samples. Comparing the one-inch and two-inch thick heat of the same carbon equivalent one can see in Figure 11 that the treatments are more effective in reducing surface hardness in the one-inch thick plate. However, the high surface hardness of this plate seems a little anomalous even without pre- or post-heat. When comparing the one-inch plates, Figure 12 shows that at the higher speed the addition of pre- and post-heat

does little more than post-heat alone, while at the slower speed the addition of pre-heat to the post-heat causes a significant additional reduction of surface hardness.

Although in this study cutting speed has only a minor effect on the hardness and toughness of the flame-cut surface, it should be noted that on production size cuts cutting speed is known to have a noticeable effect. (4) Obviously thickness and composition have a major effect. The larger thermal mass of the thicker plate extracts heat faster allowing cooling rates to exceed the critical cooling rate to form martensite deeper from the cut surface.

The one-inch thick heat 1A plate with a carbon content of 0.11% and a carbon equivalent of 0.42 is somewhat leaner in carbon than the 1B and 2A plates. This means the 1A plate has a lower hardenability, i.e., the critical cooling rate to form martensite is greater than that of the thick plate, and the hardness of the martensite which forms will be slightly lower because martensite hardness is directly proportional to carbon content.

Similar trends were also observed in the microstructures of the HAZ's. That is, the plates cut with no auxiliary heat exhibited significant quantities of martensite in the surface regions, whereas the plates cut with auxiliary pre- and post-heat exhibited softer, tempered martensite and higher temperature transformation products of bainite, pearlite and ferrite. It should be noted that experience with this auxiliary heat procedure in production size cuts has generally resulted in tempered martensite rather then bainite, pearlite and ferrite in the HAZ. (8) This microstructural difference is influenced by the smaller size of the pieces cut in this study, the rela-

tively low carbon equivalents, and the higher auxiliary heat required by the prototype equipment used.

Although difficult to resolve in the photomicrographs, Figures 13A - 13L, frequently observed was a thin layer of material that was not attacked by the 2% Nital etchant. This feature is most readily observable in Figure 13B and occurs intermittently in Figure 13C. This region generally was not found to be wider than 0.0002 in.; thus its influence on the macro properties of the flame-cut material is perhaps inconsequential. The obvious identity of this layer is that it is untempered martensite. The fact that untempered martensite does not etch well in 2% Nital would support this conclusion. However, this layer was sometimes observed in specimens which received auxiliary pre- and post-heat treatments. One would reasonably expect these treatments would temper this martensite and thus, because tempered martensite etches well with Nital, the identity of the layer is still questionable.

Because these layers are thin it is very difficult to measure their hardness in a transverse section. Nevertheless, this was attempted with some limited success by using very low loads (10 grams) in the Knoop microhardness procedure. Unfortunately, these results were inconclusive. Some samples had surface layers with hardness readings as high as 700 Knoop while others were soft, below 250 Knoop.

It is the authors' belief that these thin regions are the result of some of the molten metal resolidifying on the flame-cut surface. The reactions which occur within the flame-cut region represent very dynamic interactions between flame and metal. The chemistry of the molten metal may vary locally depending upon the local oxidizing or reducing potential of the burning gases.

Thus, it may be expected that one would find very hard, high carbon martensite or carbides at one location and soft, low carbon ferrite in another location on the same flame-cut surface.

In general, however, the microstructures are as expected. That is, in the plates cut with no auxiliary heat, at the surface (below the anomalous white layer), one observes the lower temperature transformation products. In the two-inch (51mm) thick specimens with no auxiliary heat treatment there is an area of untempered martensite at the surface. This can be seen in Figure 14, an 80X micrograph of the two-inch specimen cut at 8 inches per minute with no auxiliary heat. Here the white layer is a layer of true untempered martensite, not the anomalous thin white layer discussed above. The untempered martensite layer in Figure 14 is approximately 0.006 inch thick, significantly thicker than the anomalous layer. The hardness in this region is 550 - 450 Knoop as expected for an untempered martensite of 0.13% C. The one-inch specimens with no auxiliary heat treatment also exhibited a true untempered martensitic layer at the surface. The one and two inch specimens cut with post heat exhibited a tempered martensite/bainitic microstructure at the surface. The one-inch samples treated with auxiliary pre- and post-heat had a pearlitic microstructure at the surface, whereas the two-inch specimens treated with auxiliary pre and post heats had a bainitic/pearlitic microstructure at the surface. In all samples, as expected, the microstructure further below the surface consists of a pearlite, ferrite mixture.

Although the beneficial effects of this auxiliary heating procedure is readily evident from the above results, some circumstances have combined to make these benefits less significant then might be expected in production situations. These circumstances are the relatively low carbon equivalents and

the good toughness of A588 plates, the small sizes of the pieces cut, and the high auxiliary heat utilized due to the restrictions of the prototype equipment.

CONCLUSIONS

1) As measured by both microhardness traverses and Rockwell C surface hardness tests, a significant softening occurred in the flame-cut HAZ of 1- and 2-inch thick A588 steel plates when either auxiliary post-heat alone or pre- and post-heat together were used in the flame cutting procedure.

2) In both thicknesses, the resistance to cracking in bend testing was significantly improved by the application of auxiliary pre- and post-heat. The application of auxiliary post-heat alone also improved the bend properties although this improvement was not as significant as when both auxiliary pre- and post-heat were applied.

3) The softening effect of the auxiliary heating was dependent upon the speed of the cutting operation, whereas the performance in the bend test revealed a smaller dependence on the cutting speed.

4) The application of auxiliary heat to the flame cutting procedure was most effective in the thinner plates and at the slower cutting speeds.

5) The application of auxiliary heat in the cutting process for these materials changed the resulting microstructure in the flame-cut HAZ. Whereas untempered martensite was observed in the material cut with no auxiliary heat, none was observed in the HAZ's of the material cut with the application of auxiliary heat.

REFERENCES

1. J. A. Charles and W. J. B. Chater, "Oxygen Cutting", Metals Technology, May 1978, pp. 163-175.

2. F. Goldberg, "Influence of Thermal Cutting and Its Quality on the Fatigue Strength of Steel", Welding Journal, March 1960, pp. 229-235.

3. M. Nicolai and A. Graham, "Flame Cutting in Modern Industrial Production", Welding review, Vol. 2, No. 5, Nov. 1983, pp. 297-299.

4. A. D. Wilson, "Thermal Cutting of HSLA Bridge Steels", prepared for AISI, Final Report, August 1987.

5. R. Plecki, R. Yeske, C. Altstetter and F. V. Lawrence, Jr., "Fatigue Resistance of Oxygen Cut Steel", Welding Journal, August 1977, pp. 225s-230s.

6. N-J Ho, F.V. Lawrence, Jr. and C. J. Altstetter, "The Fatigue Resistance of Plasma and Oxygen Cut Steel", Welding Journal, November 1981, pp. 231s-236s.

7. I. A. Antonov, O. Sh. Spector and V. M. Shishlovskii, "Special Features of Thermal Processes Taking Place in the Oxygen Cutting of Heated Steel", Svar. Proiz, 1979, No. 4, pp. 1-2.

8. R. Roussey, private communication, Feb. 5, 1990.

TABLE I

CHEMICAL COMPOSITION, CARBON EQUIVALENT AND IDENTIFICATION OF THE A588 STEEL PLATES

PLATE THICKNESS HEAT NO. and ID	C	Mn	P	S	Si	Cr	V	Ni	Cu	C_{eq}
1 inch 422L7661 HEAT 1A	.11	.91	.013	.010	.32	.55	.031	.30	.30	.42
1 inch 402P6791 HEAT 1B	.13	1.23	.014	.008	.37	.54	.039	.31	.34	.49
2 inch 842526D HEAT 2A	.13	1.21	.014	.010	.43	.50	.06	.35	.33	.49

TABLE II

MECHANICAL PROPERTIES OF A588 STEEL PLATES

HEAT ID	C_{eq}	YIELD STRENGTH (KSI)	TENSILE STRENGTH (KSI)	%E in 2"	CHARPY V NOTCH (FT-LB)
1A	.42	55	76	30	185 @ 40°F
1B	.49	62.3	87.9	20	103 @ 40°F
2A	.49	69	93	21	45 @ 40°F

TABLE III

FLAME CUTTING AND AUXILIARY HEAT TREATMENT SCHEDULES

PLATE THICKNESS AND HEAT ID	CUTTING SPEED (IPM)	AUXILIARY HEAT TREATMENT NONE (NH)	POST HEAT (PH)	POST AND PRE HEAT (PPH)
1 INCH, 1A	10(S)	X	X	X
1 INCH, 1A	15(F)	X	X	X
1 INCH, 1B	10(S)	X	X	X
1 INCH, 1B	15(F)	X	X	X
2 INCH, 2A	8(S)	X	X	X
2 INCH, 2A	13(F)	X	X	X

(S) = slow; (F) = fast

TABLE IV

SUMMARY OF BEND TEST RESULTS

HEAT ID	CUTTING TREATMENT	BEND RESULTS
1A	NHS	0.5, 0.8 - 0.7 ave.
	PHS	0.7, 0.5 - 0.6 ave.
	PPHS	0.0, 0.5 - 0.3 ave.
1A	NHF	0.7, 0.8 - 0.8 ave.
	PHF	0.5, 0.5 - 0.5 ave.
	PPHF	0.0, 0.0 - 0.0 ave.
1B	NHS	1.6, 1.5, 1.8, 2.0 - 1.7 ave.
	PHS	1.0, 1.0, 1.0, 0.7 - 0.9 ave.
	PPHS	0.4, 0.5, 0.5, 0.0 - 0.3 ave.
1B	NHF	1.8, 1.2, 2.0, 1.5 - 1.6 ave.
	PHF	1.0, 1.0, 0.7, 1.0 - 0.9 ave.
	PPHF	0.0, 0.0, 0.5, 0.0 - 0.1 ave.
2A	NHS	2.0, 2.0 - 2.0 ave.
	PHS	1.0, 1.0 - 1.0 ave.
	PPHS	0.7, 0.8 - 0.8 ave.
2A	NHF	2.0, 2.0 - 2.0 ave.
	PHF	2.0, 2.0 - 2.0 ave.
	PPHF	0.8, 1.0 - 0.9 ave.

TABLE V

TYPICAL STATISTICAL VARIATION OF THE
KNOOP MICROHARDNESS DATA

	DISTANCE FROM THE FLAME CUT EDGE, mm				
	0.1	0.3	0.5	2.5	5.0
MEAN	490	455	430	277	246
RANGE	148	163	194	68	56
STD. DEVIATION	58	64	76	27	22

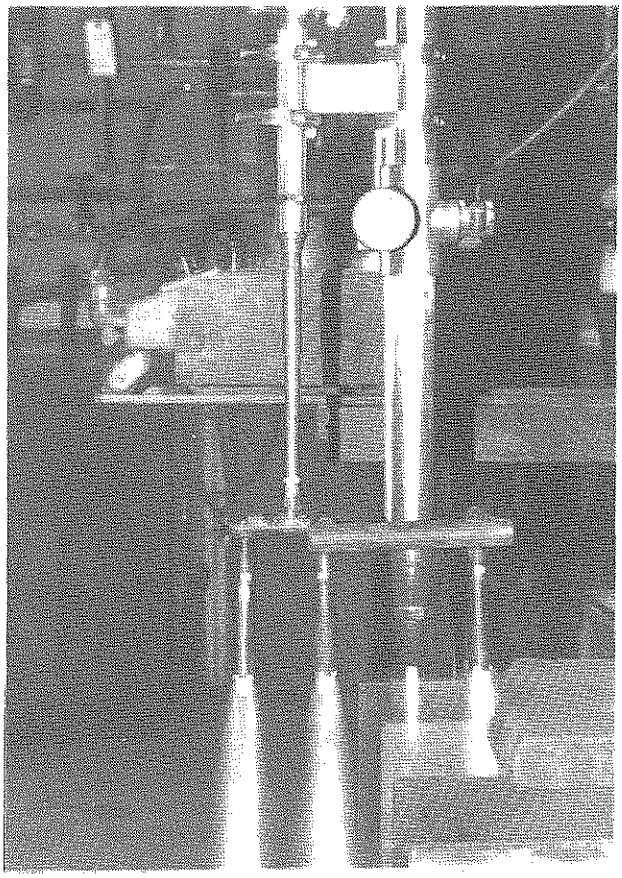

Figure 1: Photograph showing arrangement of auxiliary heat flame cutting fixture.

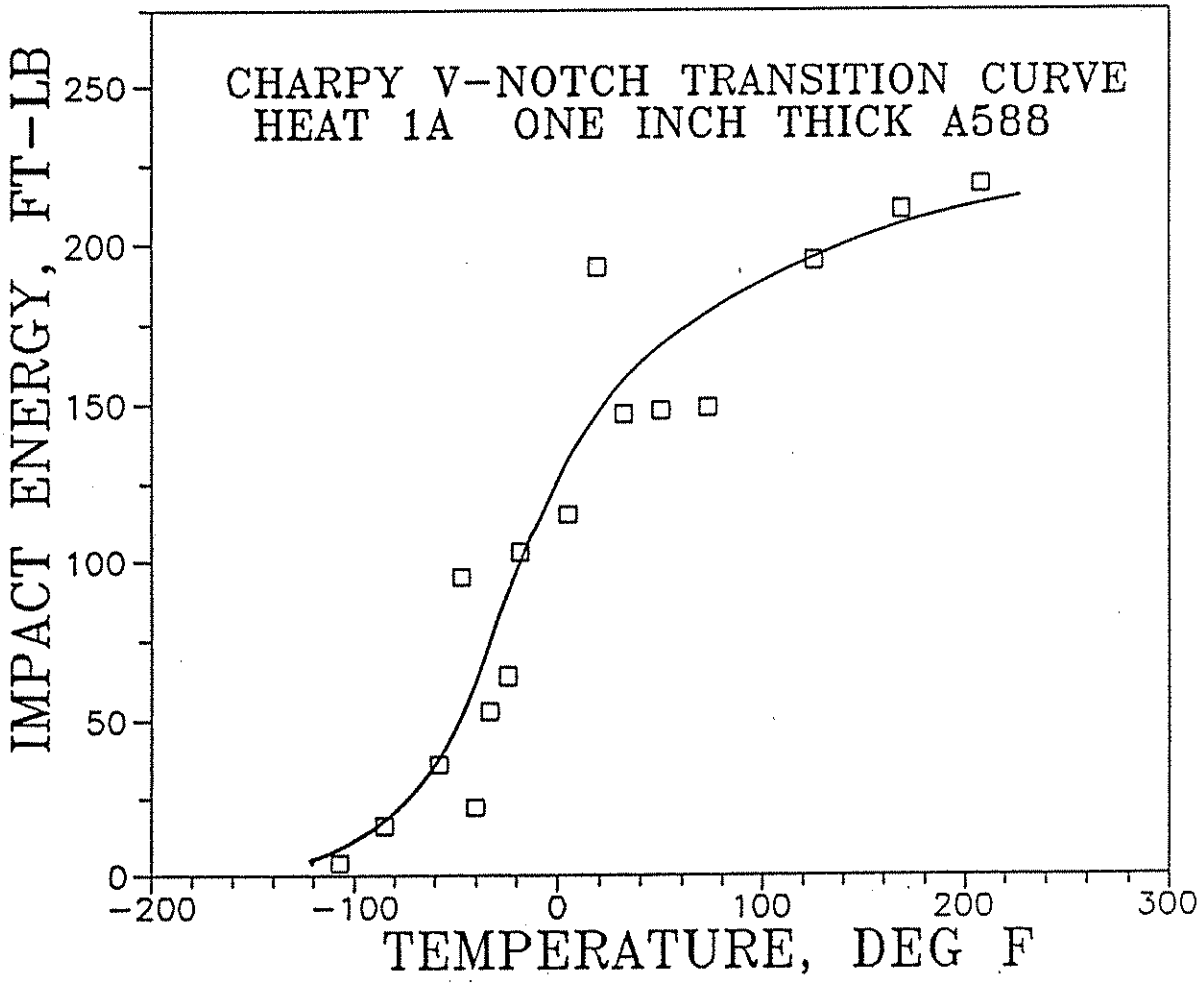

Figure 2: Charpy V-Notch transition curve for Heat 1A, one inch thick A588 plate with carbon equivalent of 0.42.

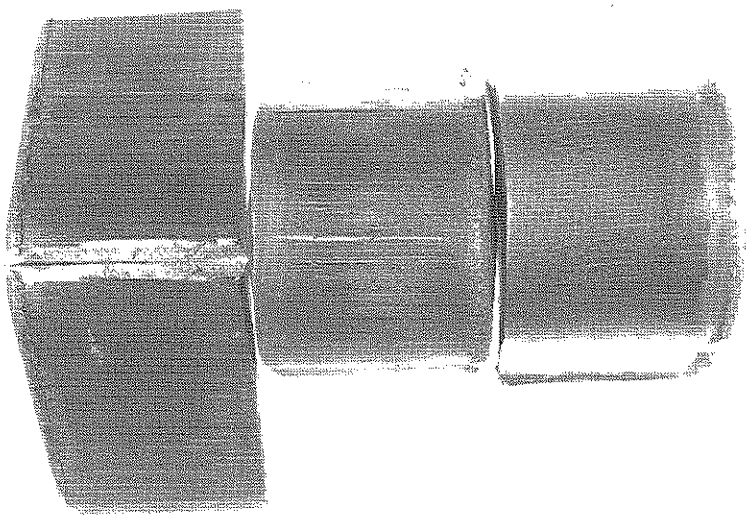

Figure 3: Bend specimens from 2 inch thick A588 steel cut at 8 inches per minute. Specimen on left cut with no auxiliary heat shows through crack (2.0 rating). Specimen in middle cut with auxiliary post heat shows major crack (1.0 rating). Specimen on right cut with auxiliary pre- and post-heat shows numerous slight cracks (0.7 rating).

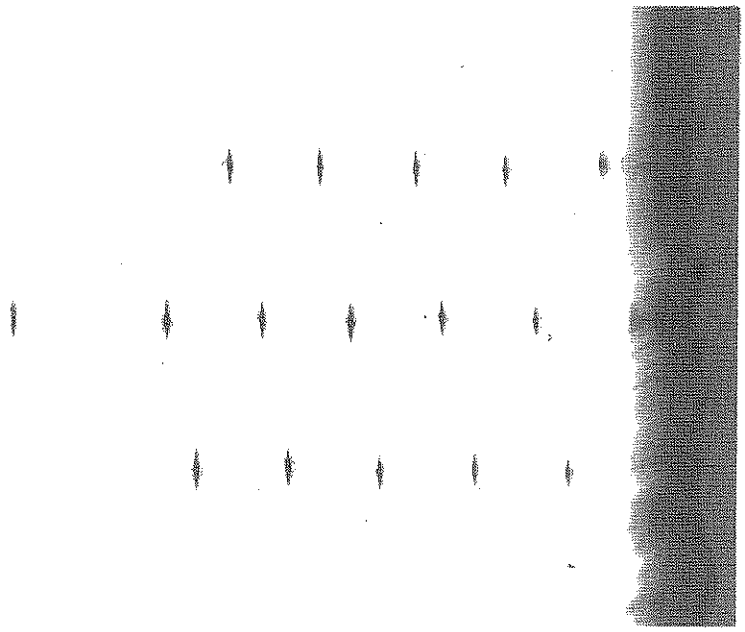

Figure 4: Photomicrograph showing sequence of Knoop hardness indentations at flame-cut surface. Flame-cut surface at right.

As-polished Magnification: 80X

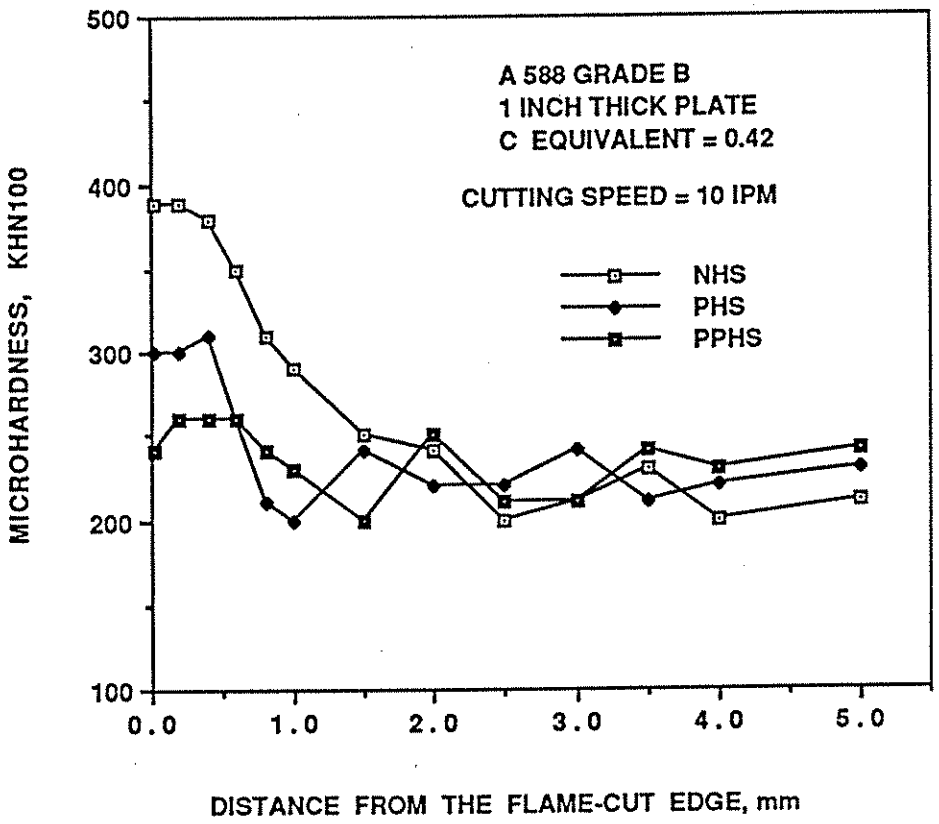

Figure 5: Microhardness survey for one inch thick A588 plate Heat 1A cut at 10 inches per minute

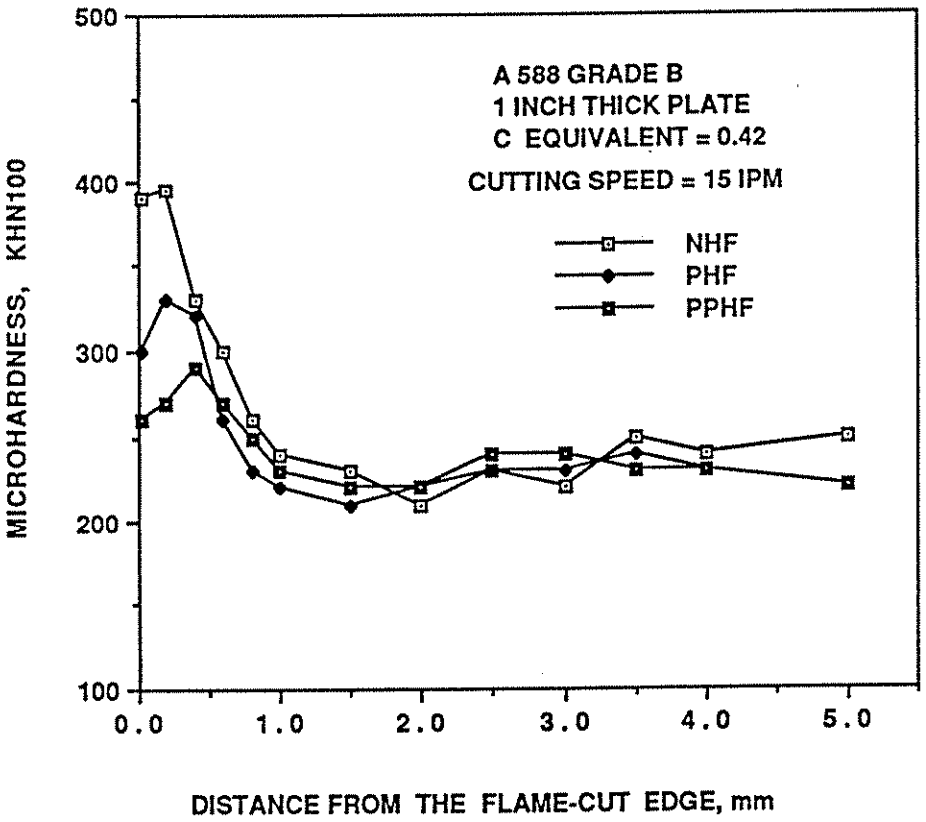

Figure 6: Microhardness survey for one inch thick A588 plate Heat 1A cut at 15 inches per minute

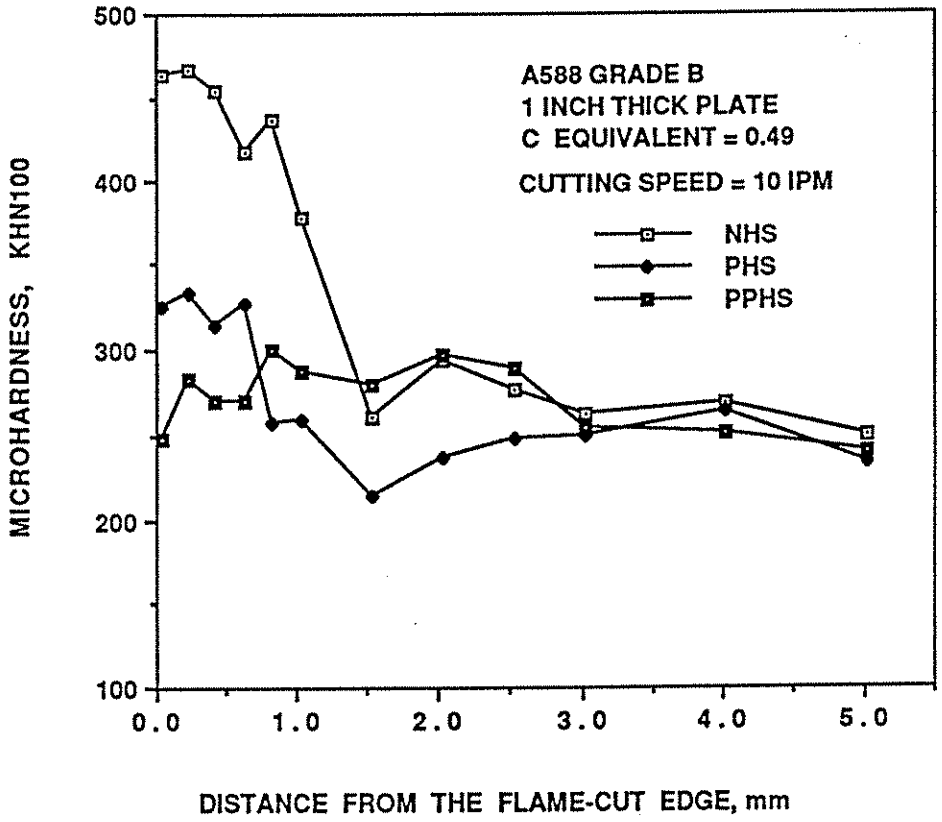

Figure 7: Microhardness survey for one inch thick A588 plate Heat 1B cut at 10 inches per minute

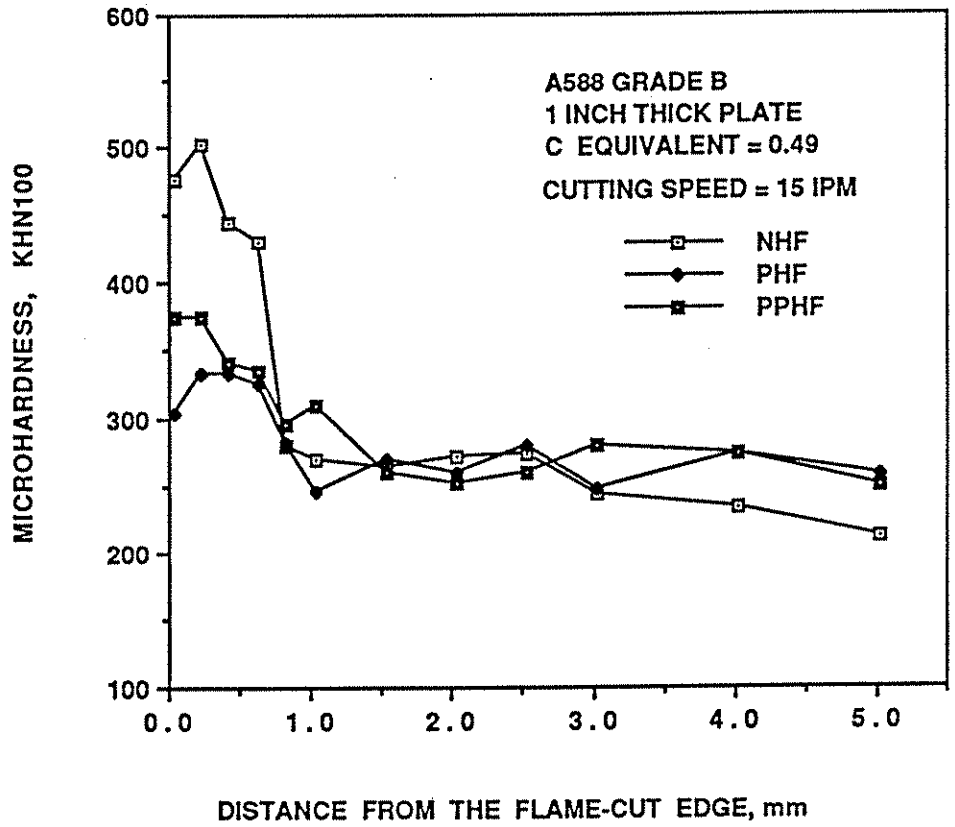

Figure 8: Microhardness survey for one inch thick A588 plate Heat 1B cut at 15 inches per minute

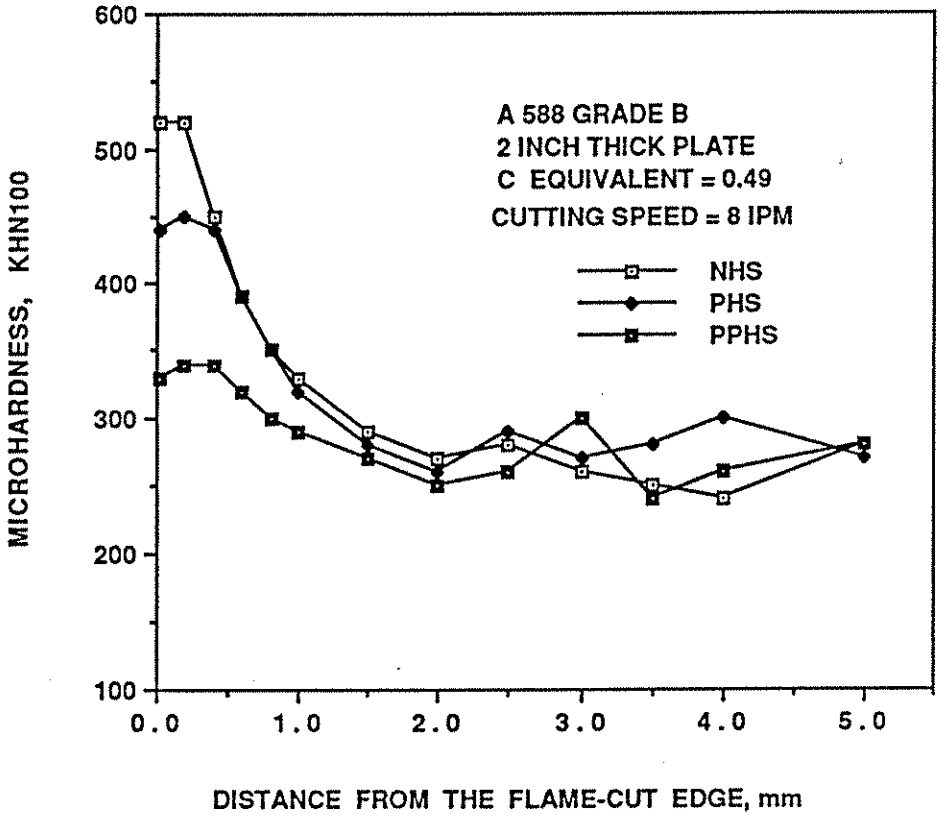

Figure 9: Microhardness survey for two inch thick A588 plate Heat 2A cut at 8 inches per minute

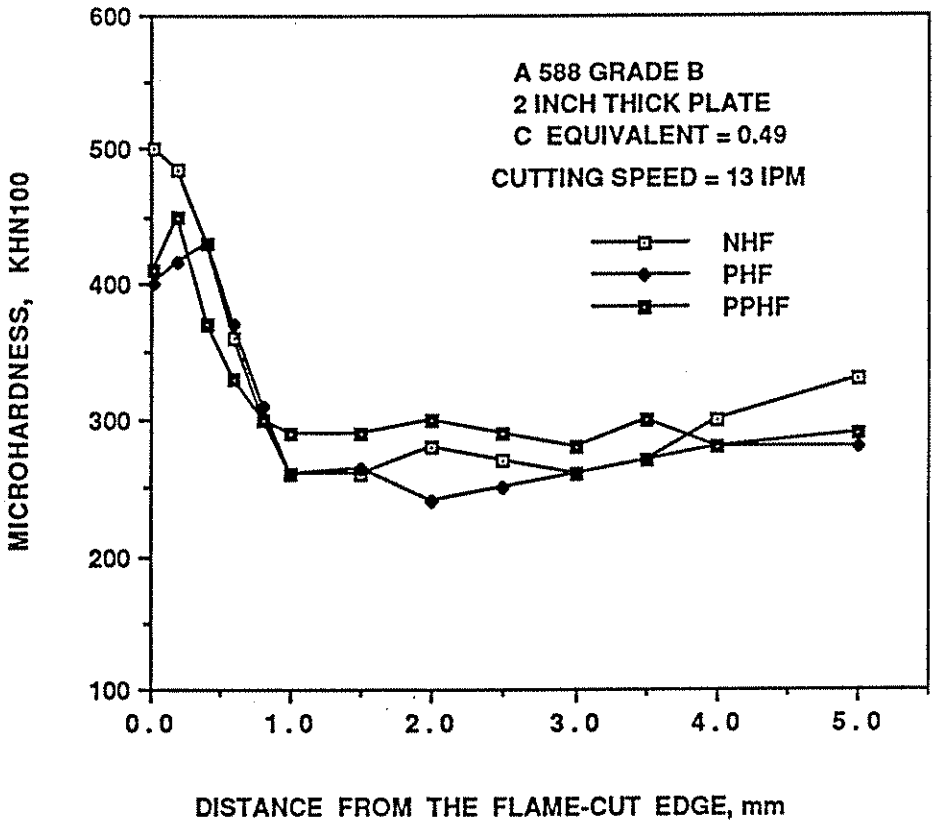

Figure 10: Microhardness survey for two inch thick A588 plate Heat 2A cut at 13 inches per minute

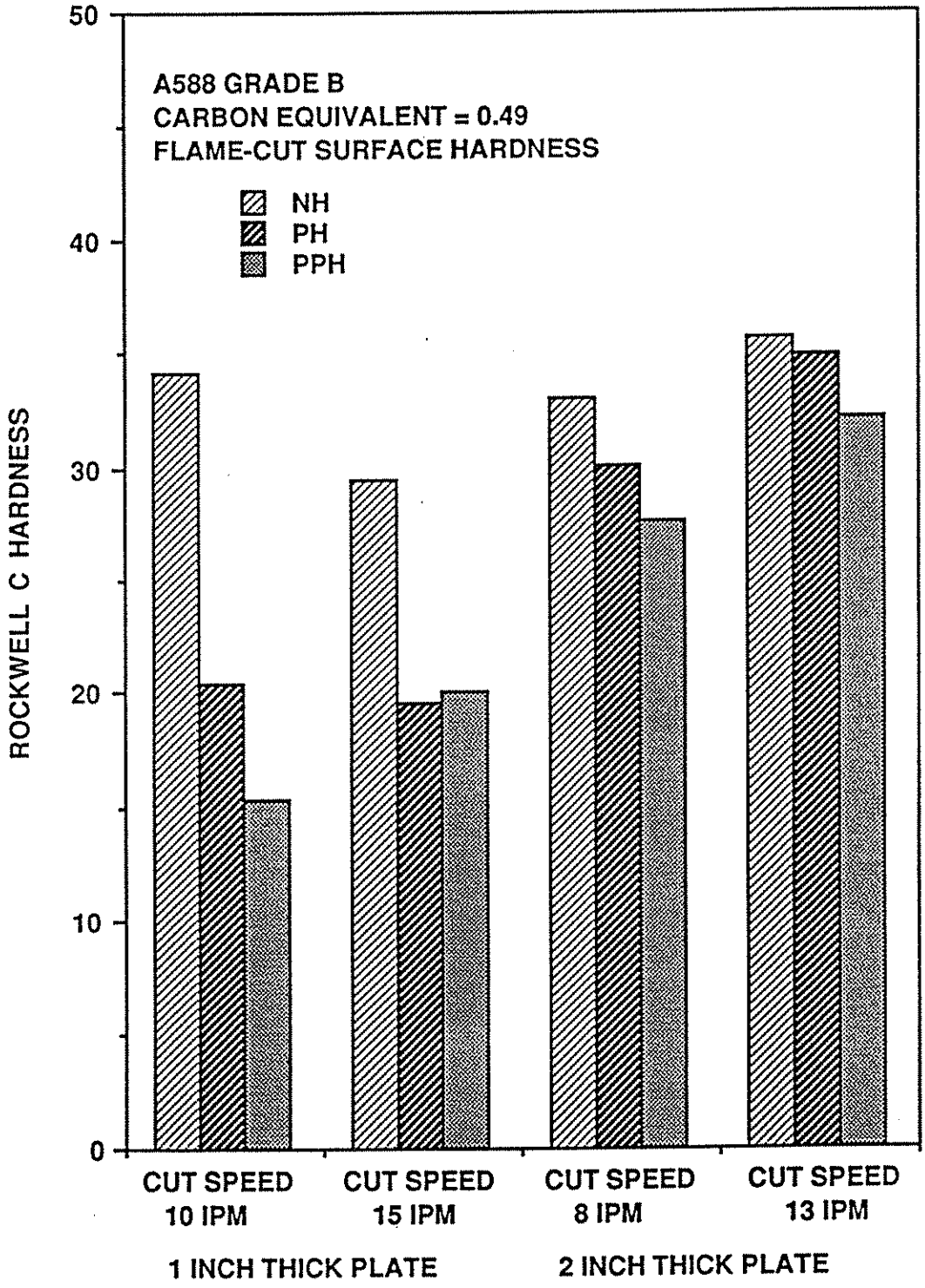

Figure 11: Flame cut surface hardness of one inch, Heat 1B and two inch, Heat 2A, A588 steel plates of similar carbon equivalent.

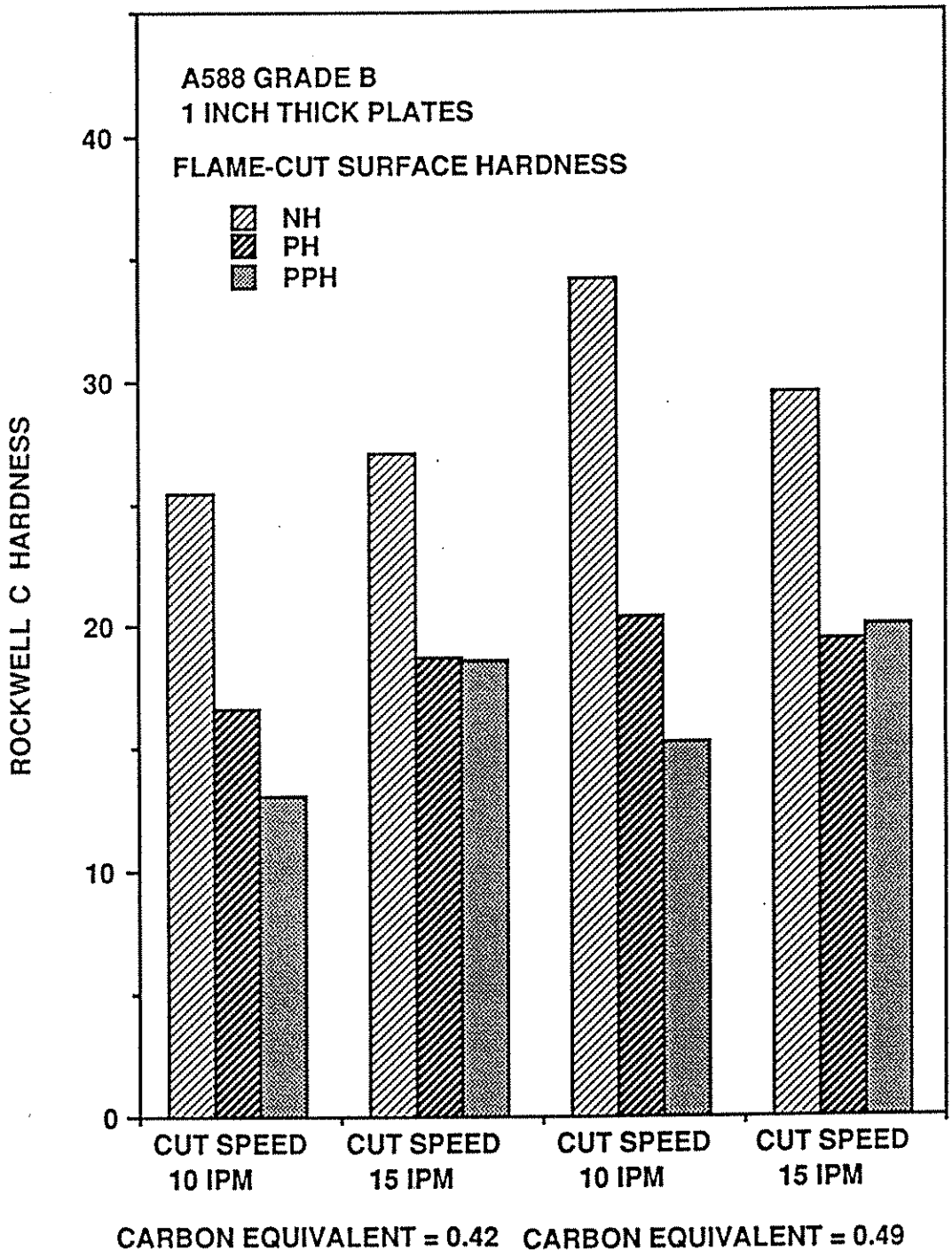

Figure 12: Flame cut surface hardness of one inch, Heat 1A and Heat 1B, A588 steel plates.

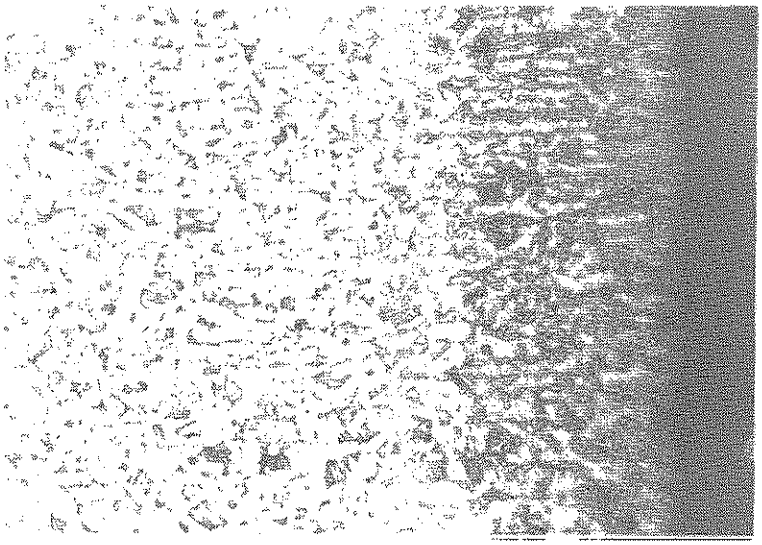

A) No Auxiliary Heat

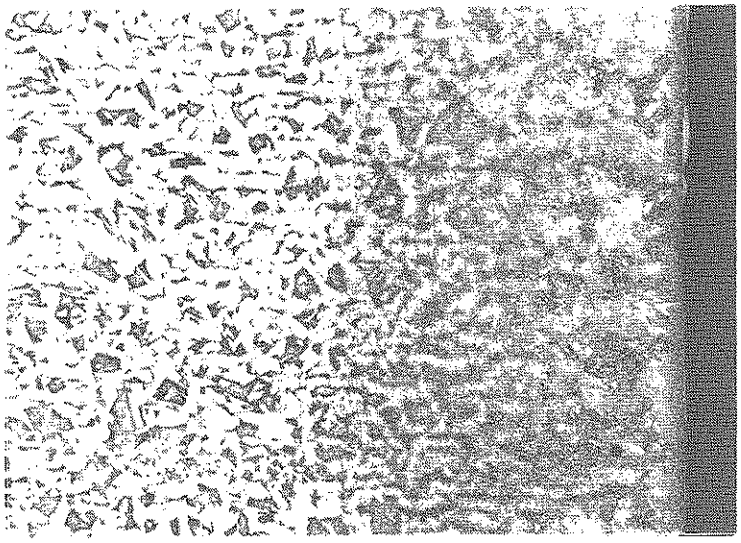

B) Post Heat

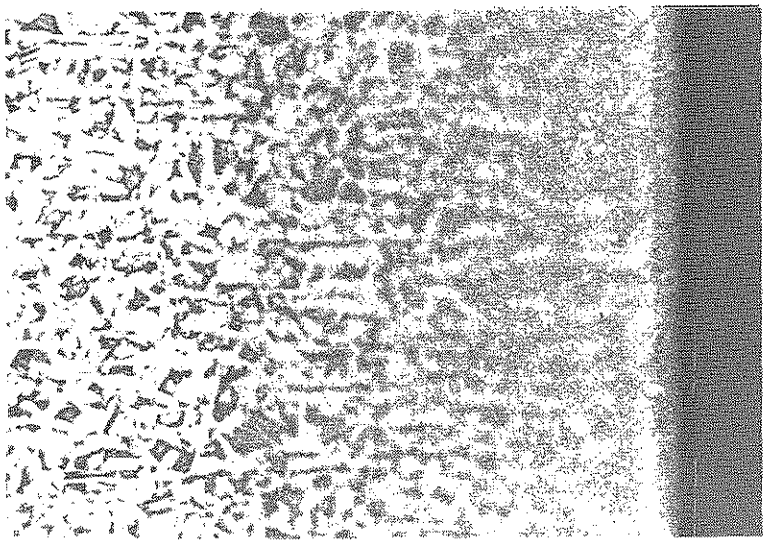

C) Post and Pre Heat

Figure 13 (A-C): Optical photomicrographs showing microstructure of HAZ in one inch thick flame-cut A588 steel cut at 15 inches per minute.
Etchant: 2% Nital Magnification: 40X

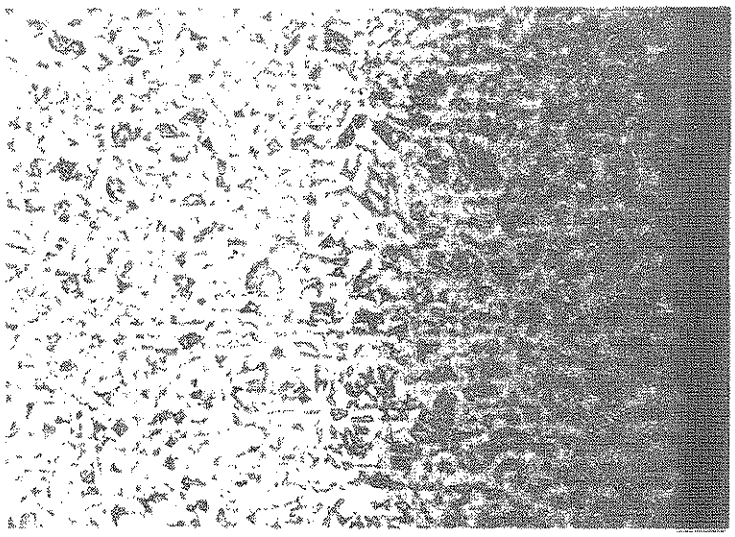

D) No Auxiliary Heat

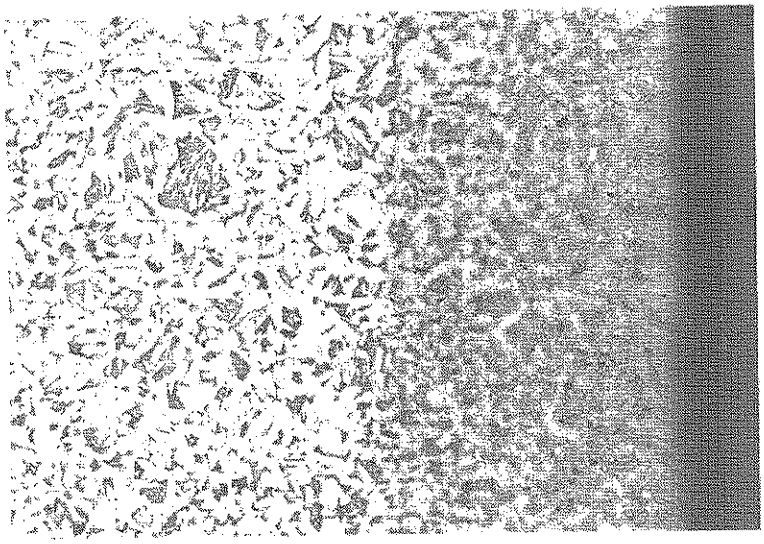

E) Post Heat

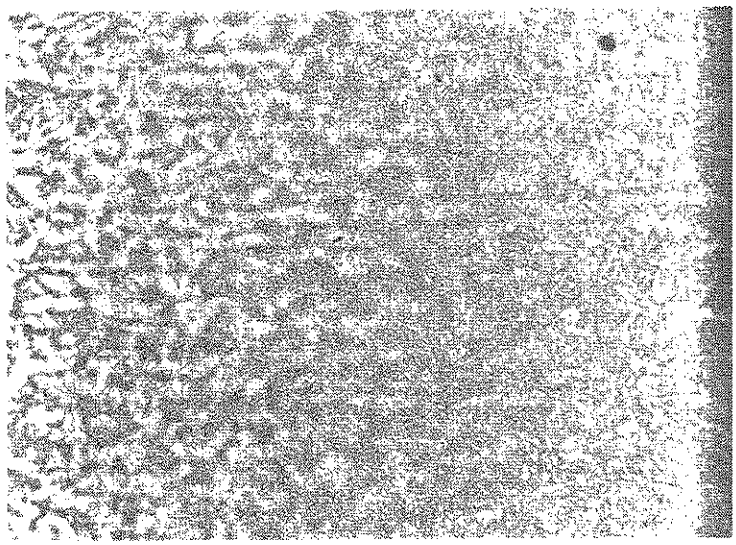

F) Post and Pre Heat

Figure 13 (D-F): Optical photomicrographs showing microstructure of HAZ in one inch thick flame-cut A588 steel cut at 10 inches per minute.
Etchant: 2% Nital Magnification: 40X

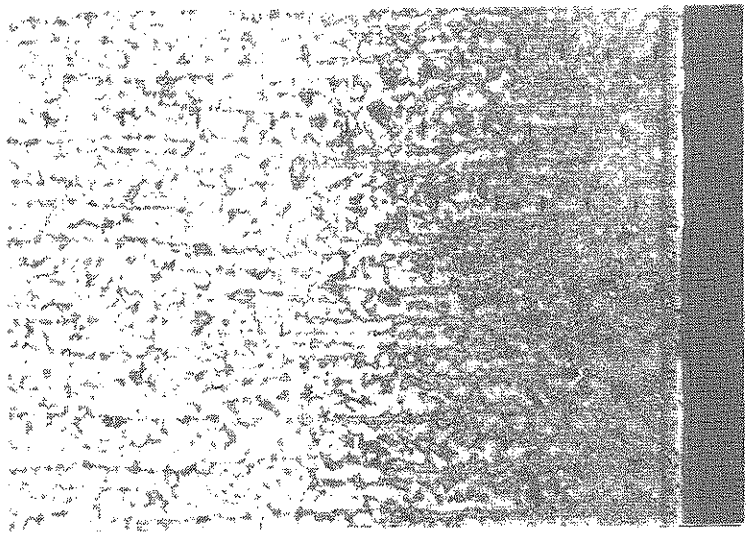

G) No Auxiliary Heat

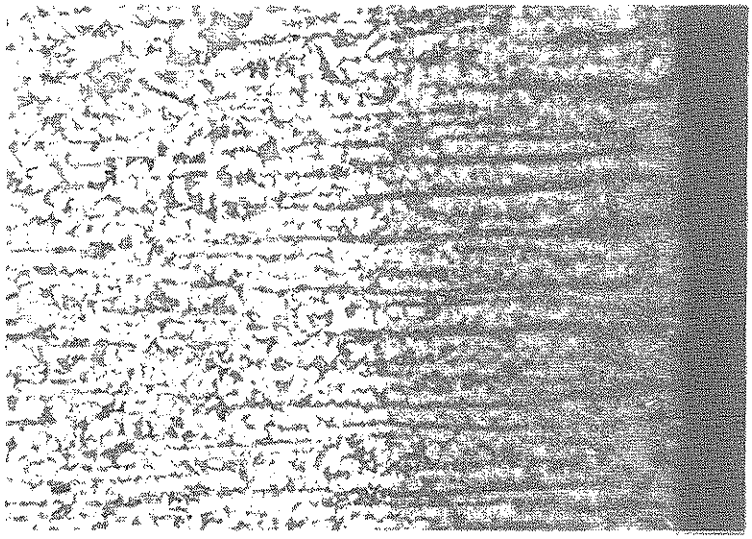

H) Post Heat

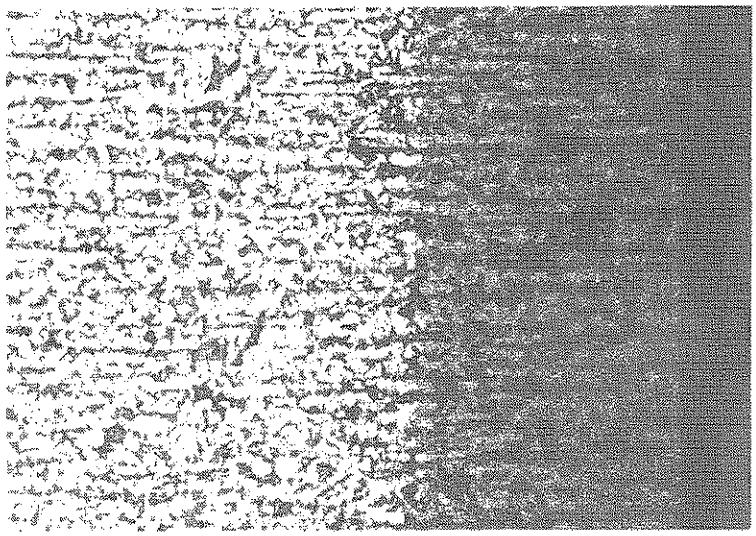

I) Post and Pre Heat

Figure 13 (G-I): Optical photomicrographs showing microstructure of HAZ in two inch thick flame-cut A588 steel cut at 13 inches per minute.
Etchant: 2% Nital Magnification: 40X

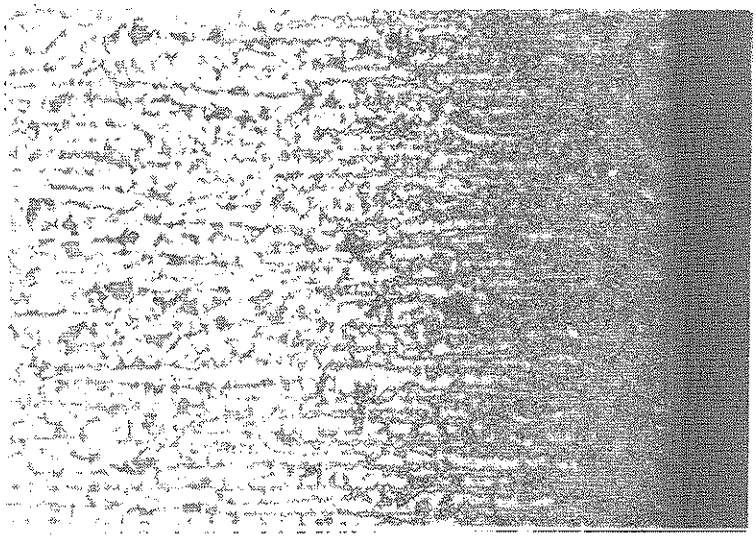

J) No Auxiliary Heat

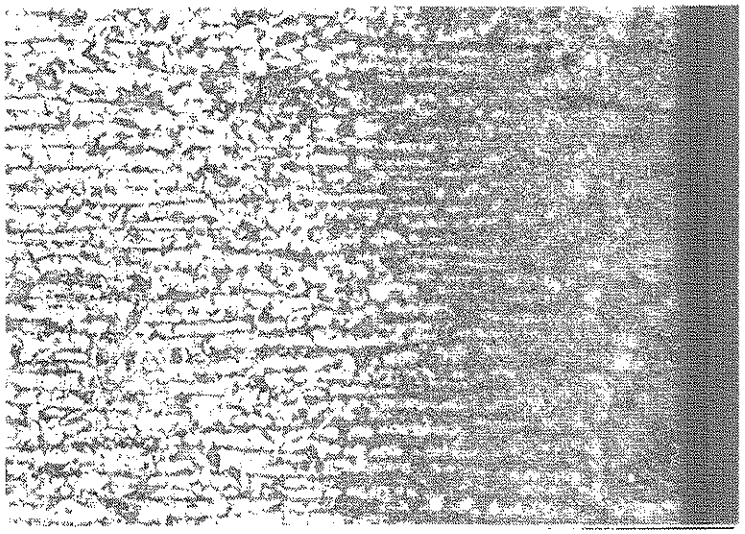

K) Post Heat

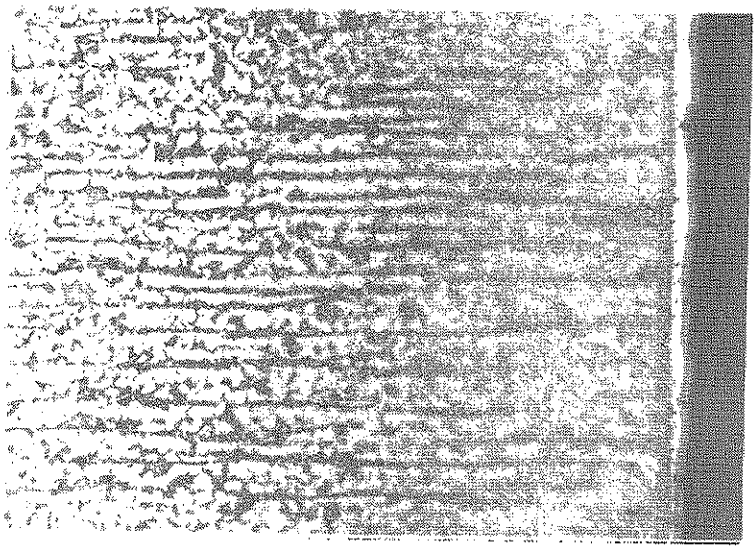

L) Post and Pre Heat

Figure 13 (J-L): Optical photomicrographs showing microstructure of HAZ in two inch thick flame-cut A588 steel cut at 8 inches per minute.
Etchant: 2% Nital Magnification: 40X

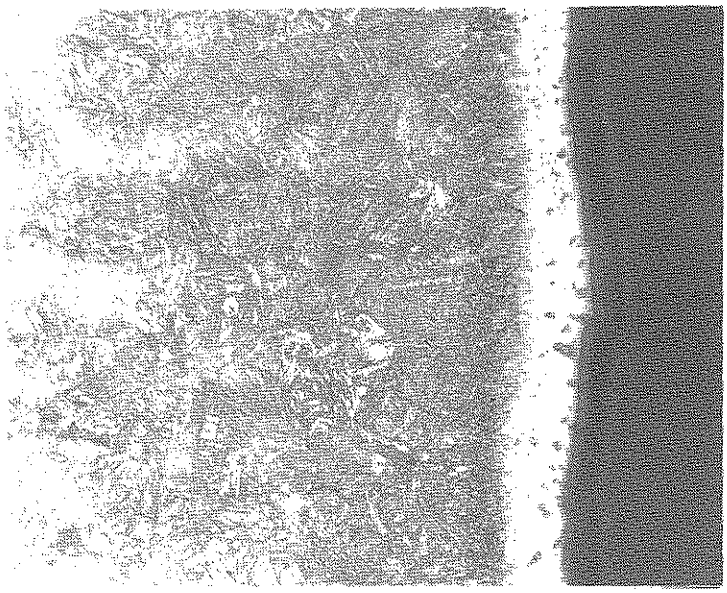

Figure 14: Optical photomicrograph of a HAZ cross-section in the two inch thick A588 steel plate cut with no auxiliary heat at 8 inches per minute. Note the unetched layer of martensite at the flame-cut surface (on right).
Etchant: 2% Nital Magnification: 80X